SMC-TR-98-10

AEROSPACE REPORT NO.
TR-94(4935)-2

Fiber Strength Utilization in Carbon/Carbon Composites: Part II. Extended Studies With Pitch- and PAN-Based Fibers

15 January 1998

Prepared by

R. J. ZALDIVAR and G. S. RELLICK
Mechanics and Materials Technology Center
Technology Operations

J-M Yang
Department of Materials Science and Engineering
University of California, Los Angeles

Prepared for

SPACE AND MISSILE SYSTEMS CENTER
AIR FORCE MATERIEL COMMAND
2430 E. El Segundo Boulevard
Los Angeles Air Force Base, CA 90245

Engineering and Technology Group

THE AEROSPACE CORPORATION
El Segundo, California

This report was submitted by The Aerospace Corporation, El Segundo, CA 90245-4691, under Contract No. F04701-93-C-0094 with the Space and Missile Systems Center, 2430 E. El Segundo Blvd., Los Angeles Air Force Base, CA 90245. It was reviewed and approved for The Aerospace Corporation by S. Feuerstein Principal Director, Mechanics and Materials Technology Center. Maj. J. W. Cole was the project officer for the Mission-Oriented Investigation and Experimentation (MOIE) program.

This report has been reviewed by the Public Affairs Office (PAS) and is releasable to the National Technical Information Service (NTIS). At NTIS, it will be available to the general public, including foreign nationals.

This technical report has been reviewed and is approved for publication. Publication of this report does not constitute Air Force approval of the report's findings or conclusions. It is published only for the exchange and stimulation of ideas.

MAJ. J. W. COLE
SMC/AXES

REPORT DOCUMENTATION PAGE

Form Approved
OMB No. 0704-0188

1. AGENCY USE ONLY (Leave blank)	2. REPORT DATE	3. REPORT TYPE AND DATES COVERED
	15 January 1997	

4. TITLE AND SUBTITLE
Fiber Strength Utilization in Carbon/Carbon Composites: Part II. Extended Studies With Pitch- and PAN-Based Fibers

5. FUNDING NUMBERS
F04701-93-C-0094

6. AUTHOR(S)
R. J. Zaldivar and G. S. Relick

7. PERFORMING ORGANIZATION NAME(S) AND ADDRESS(ES)
The Aerospace Corporation
Technology Operations
El Segundo, CA 90245

8. PERFORMING ORGANIZATION REPORT NUMBER
TR-94(4935)-2

9. SPONSORING/MONITORING AGENCY NAME(S) AND ADDRESS(ES)
Space and Missile Systems Center
Air Force Materiel Command
2430 E. El Segundo Blvd.
Los Angeles Air Force Base, CA 90245

10. SPONSORING/MONITORING AGENCY REPORT NUMBER
SMC-TR-98-10

11. SUPPLEMENTARY NOTES

12a. DISTRIBUTION/AVAILABILITY STATEMENT
Approved for public release; distribution unlimited

12b. DISTRIBUTION CODE

13. ABSTRACT (Maximum 200 words)

Meaurements of fiber strength utilization (FSU) in unidirectional carbon/carbon (C/C) composites as a function of heat-treatment temperature (HTT) have been extended beyond the original group of DuPont pitch-based E-series fibers to include additional pitch- and PAN-based fibers. Fibers and composites were characterized by tensile strength, optical microscopy, SEM, fiber preferred orientation, and a single-fiber composite (SFC) fragmentation test to provide a relative measure of fiber-matrix interfacial shear strength (IFSS). Results show that fracture behavior and FSU are dominated by the degree of fiber-matrix bonding, as inferred from microscopic observations and measurements of IFSS. In the very high modulus pitch-based fibers, the behavior of the E130 is strikingly different from that of the Amoco and Nippon Oil fibers, in that it retains good bond strength and high FSU even with HTT to 2400°C, in contrast to the other very high modulus pitch-based fibers that are already weakly bonded at the lowest HTT of 1100°C. All PAN-based fibers and lower modulus pitch fibers are characterized by strong bonding, brittle fracture, and low FSU for the 1100°C HTT. Subsequent heat treatment of these composites to 2150 and 2400°C, in most cases, results in significant recovery of FSU, suggesting an optimum IFSS for each composite. It is suggested that the difference in bonding between the pitch-based E-series and P-series may be related to the similarity in fine structure between the E-fibers and high-modulus PAN-based fibers.

14. SUBJECT TERMS
Composites, Carbon-carbon, carbon fibers

15. NUMBER OF PAGES
16

16. PRICE CODE

17. SECURITY CLASSIFICATION OF REPORT	18. SECURITY CLASSIFICATION OF THIS PAGE	19. SECURITY CLASSIFICATION OF ABSTRACT	20. LIMITATION OF ABSTRACT
UNCLASSIFIED	UNCLASSIFIED	UNCLASSIFIED	

Preface

This work was performed under United States Air Force Contract No. F04701-88-C-0089. The authors thank Mr. Paul Adams of The Aerospace Corporation for performing the X-ray diffraction measurements. One of us (RJZ) thanks The Aerospace Corporation for financial support in the form of a Corporate Fellowship.

Contents

Figures

Tables

I. INTRODUCTION

In a previous study,[1] we reported on the fiber utilization (FSU) in single-tow unidirectional carbon/carbon (C/C) composites of a series of DuPont mesophase-derived carbon fibers E35, E75, E105, and E130 as a function of composite heat-treatment temperature (HTT). The number in the fiber designates its nominal modulus in units of Mpsi. FSU is defined as the ratio of apparent fiber strength in the C/C composite to the fiber strength in a baseline resin-matrix composite. The C/C composite matrix precursor was polyarylacetylene (PAA), which is a high-char-yield thermoset resin derived from polymerization of diethynylbenzene. Its chemistry and use as a matrix precursor in C/C's is discussed in more detail elsewhere.[2,3]

In the earlier study,[1] it was found that the 1100 °C HTT (carbonization) results in a brittle carbon matrix that bonds strongly with the three lower-modulus fibers. The result is matrix-dominated failure at failure strains well below those of the fibers, and therefore, low FSU values in the composite (24 to 35%). However, the E130 fiber composite had a much higher FSU of 79%. Part of this higher FSU in the E130 can be attributed to the much lower-failure strain of the E130 fiber relative to the other three fibers (see Ref. 1), which factor, acting alone, works to reduce the discrepancy between matrix and fiber failure strains and, therefore, favors better utilization of fiber strength. Another way of stating this is as follows: If in a series of composites made up of fibers of different moduli, the composite failure strain in each case is equal to the matrix failure strain, and the fiber failure strains decrease with increasing fiber moduli, which is typically the case (e.g., Ref. 1) then the FSU in the composites will increase with fiber modulus. A much larger factor for the E130 composite, however, was that the failure strain was significantly higher than those of the E75 and E105 composites (0.20 vs 0.09 and 0.11). SEM examinations of the composite fracture surfaces revealed two significant features. The first was that the E130 composite had measurable fiber pullout, indicative of a weaker fiber-matrix interface. Such fiber-matrix interface weakening works to deflect the propagation of brittle-matrix cracks and improve composite strength. The second feature, which may have also contributed to the higher E130 composite failure strain and FSU, was tough fracture of the filaments themselves. Each E130 filament revealed an irregular, jagged fracture path, unlike the other three lower-modulus filaments, which all revealed smooth fracture surfaces.

For the three lower-modulus fibers, heat treatment to 2150 and 2400 °C led to a significant recovery of composite strength as a consequence of interface weakening, once again inferred from SEM fractographs showing fiber pullout. Heat treatment to 2750 °C led to large decreases in FSU for all the composites in spite of significant strength increases in the heat-treated bare fibers. One factor in this strength decrease was long-range matrix decohesion, which results from extensive graphitization of the matrix. A second, and probably more significant, factor was physical degradation of the fiber *in the composite* as a result of the large thermochemical stresses generated as a result of such a high HTT.

In more recent work,[4] we have studied the tensile fracture behavior of the E130 composite in finer detail by employing a portable flexure stage in an SEM. One interesting observation in this study was that of multiple matrix cracking in the 2150 °C HTT samples. More specifically, we observed the formation of evenly spaced multiple matrix cracks bridged by intact fibers. This behavior is predicted for brittle-matrix composites by the now-classic theory of Aveston, Cooper, and Kelly,[5] and is essentially identical to that observed in the SiC/glass-ceramic composites studied by Marshall and Evans[6] and the SiC/lithium aluminosilicate (LAS) composite studied by Barsoum *et al.*[7] It is perhaps significant that the maximum FSU of 92% for the E130 composite[1] corresponds to the HTT (2150 °C) at which multiple matrix cracking is observed; at the same time, we studied only four HTT's and so cannot rule out the formation of multiple matrix cracks over a range of HTT's.

In the current work, we continue out studies of fiber tensile strength utilization in C/C's. We have extended the number and type of fibers studied beyond the four DuPont fibers to include mesophase-pitch-based fibers from Amoco and Nippon Oil, and PAN-based fibers from Amoco and Hercules. Table I provides a list of fibers used in the current and previous[1] study. The fibers selected give us the opportunity to study the influence of fiber type and microstructure on the composite tensile strengths.

TABLE I. List of fibers studied.

Fiber	Fiber precursor	Manufacturer
E35[a]	Mesophase pitch	DuPont
E75[a]		
E105[a]		
E130[a]		
P55		Amoco
P100		
PX7		
XN70		Nippon Oil
T50	PAN	Amoco
UHMS		Hercules
IM6		
IM7		

[a]Fibers used in previous study.[1]

II. EXPERIMENTAL PROCEDURES

Procedures of single-tow specimen fabrication and tensile testing are described in detail in our previous publication.[1] In the current work, we have also employed two additional characterization techniques. The first is a single-fiber-composite (SFC) fragmentation test, which provides a measure of fiber-matrix interfacial shear strength (IFSS) for a given fiber and matrix combination. In this technique, a dogbone specimen is prepared with a single fiber embedded in a compliant matrix. The fiber is aligned along the centerline of the dogbone, which is loaded in tension along the fiber axis. As the strain in the specimen increases with the applied load, the fiber breaks in tension repeatedly at weak points along its length. The fragmentation process continues until the fiber fragment reaches a minimum final length, termed the "critical length," l_c, at which no further fragmentation is possible because the fragment lengths are so short that the shear stress transfer along their lengths cannot build up enough tensile stresses to cause further failures.

Kelly and Tyson[8] were the first to use this approach to estimate the IFSS of brittle tungsten fibers embedded in a copper matrix. Using a force balance approach, they showed that an average IFSS, τ, can be calculated from

$$\tau = \frac{\sigma_f}{2}\left(\frac{d}{l_c}\right), \tag{1}$$

where σ_f is the fiber strength, and d is the fiber diameter.

Since, in principle, any fragment of length just slightly greater than l_c can also fracture, the lower bound for fragment lengths is $l_c/2$, and there will be a distribution of fragment lengths between $l_c/2$ and l_c. It is common to relate l_c to the experimentally measured average of final fragment lengths, $\bar{l}$, by $\bar{l} = 0.75\ lc$. This leads to the modified equation:

$$\tau = 0.75\ \frac{\sigma_f}{2}\left(\frac{d}{l}\right), \tag{2}$$

This technique has been used extensively by Drzal and co-workers[9–11] to characterize the IFSS of various carbon fibers in epoxy matrices. They have also refined the micromechanical analyses using Weibull statistics to account for distributions of fiber strengths and fragment lengths. In our work, we used Eq. (2) and the average fiber strengths measured from our standard 2 in. gauge-length resin-impregnated strands[1] and nominal fiber diameters reported by the manufacturers. A more rigorous treatment of the problem requires the use of single filament testing to obtain the fiber strength corresponding to l_c. As a result, our use of 2 in. gauge-length strengths probably underestimates the IFSS values somewhat. However, given the wide variation in IFSS values obtained by various test techniques[11] and different resin matrices, it is clear that the principal value of the technique is in providing a relative ranking of bond strengths of fibers in a given matrix.

For the fabrication of the single-fiber composite specimens, an epoxy resin (Shell EPON 815) was mixed with a standard curing agent catalyst (diethylenetriamine, obtained from Johnson Matthey Electronics). A ratio of 16 : 1 was used. The epoxy solution was stirred at room temperature to form a homogeneous mixture, which was degassed in a vacuum chamber. The solution was then poured into flat Teflon dogbone molds, in which single carbon fibers had been positioned under slight tension. The epoxy solution was cured in air for 16 h, and the dogbones were removed and tested under tension using a manually controlled straining stage.

The second new characterization we employed was the measurement of fiber preferred orientation. Measurement of the full width at half maximum (FWHM) of the azimuthal intensity of the (002) reflection was made for us by Adams using a flat-film x-ray diffraction (XRD) technique developed by Adams and described in detail elsewhere.[12] Basically, this technique involves the use of image analysis technology to extract, store, manipulate, and analyze the information contained in pinhole photographs of carbon fibers made with nickel-filtered copper radiation in a flat-film plate camera.

III. RESULTS AND DISCUSSION

Table II lists selected properties for the as-received fibers. Modulus values on our 2 in. gauge-length resin strands agree well with manufacturers' reported values. However, agreement among strength values is not expected to be as good because the measurement of fiber strength is sensitive to test technique (e.g., single filament versus strand) and test condition (e.g., gauge length), and these vary among the manufacturers. Lot-to-lot variations may also account for significant differences in reported fiber strengths. Nevertheless, Table II reveals that the overall agreement with the variously reported strengths is good. For the four PAN fibers, the agreement is excellent. For the E-series fibers, our strengths are consistently about 15–20% lower than those reported by DuPont for 6 in. epoxy resin strands.[1] Possible reasons for this are discussed in Ref. 1. Agreement is good for the P55 and P100 fibers, but for the PX7, our strength is about 20% less than reported for the nominally similar P130X in Ref. 13. Little of the experimental-grade PX7 fiber was made by Amoco, and we were unable to obtain strength data on our particular lot. The largest discrepancy in strength is with the XN70 fibers, but we have the least information on this fiber from Nippon Oil. However, our measured strength of 2.1 GPa for XN70 is in the same range of values found for the other mesophase-based fibers. Note that only the three Hercules fibers were surface treated, and only the XN70 and T50 were sized.

Figures 1 and 2 are plots of FSU versus HTT for the pitch- and PAN-based fibers, respectively. As before, 100% FSU is defined as the fiber strength in the cured-resin composite. In this and the heat-treated C/C composites, the load carried by the matrix is ignored since $E_m V_m \ll E_f V_f$; the fiber strength, S_f, is then calculated from $S_f = P_c^u / A_f$, where P_c^u is the breaking load

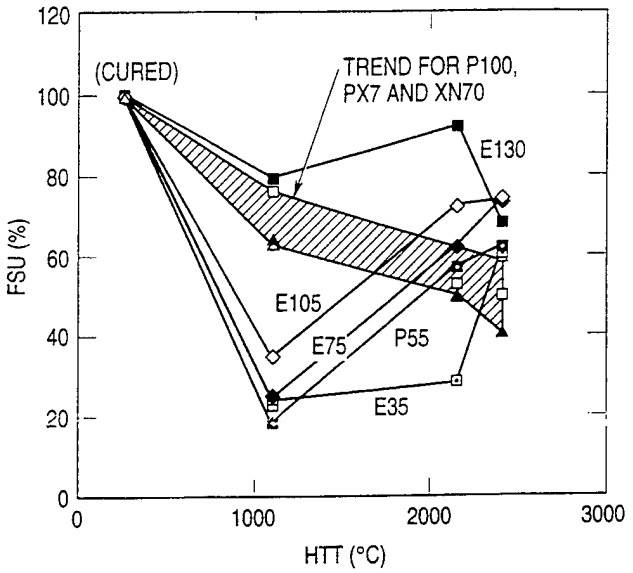

FIG. 1. Fiber strength utilization (FSU) versus heat-treatment temperature (HTT) for pitch-based fibers. Shaded area shows trend for P100, PX7, and XN70 fibers.

TABLE II. Selected properties of as-received fibers.

Fiber	Diameter (μm)	Filaments per tow	Modulus (GPa)		Strength (GPa)		Surface treatment/sizing
			Manufacturer	Present work[f]	Manufacturer	Present work[f]	
E35	9.2[a]	3.000	241[a]	240	2.5[g]	2.0	No/No
E75	9.6[a]	3.000	517[a]	517	2.4[g]	2.1	No/No
E105	9.6[a]	3.000	724[a]	758	2.6[g]	2.1	No/No
E130	10.0[a]	3.000	897[a]	827	2.7[g]	2.3	No/No
P55	11[b]	4.000	379[b]	377	1.9[b]	1.8	No/No
P100	10[b]	2.000	765[b]	724	2.4[b]	2.2	No/No
PX7	11[b]	3.000	923[b]	897	2.9[b]	2.3	No/No
XN70	10[c]	3.000	690[c]	...	3.3[c]	2.1	No/Yes
T50	6.5[d]	3.000	393[d]	380	2.4[d]	2.4	No/Yes
UHMS	4.5[e]	12.000	435[e]	415	3.8[e]	3.6	Yes/No
IM6	5.0[e]	12.000	276[e]	270	5.1[e]	5.0	Yes/No
IM7	5.0[e]	12.000	272[e]	260	5.4[e]	5.2	Yes/No

[a]Product data sheets. Properties are nominal as reported by DuPont.
[b]Reported in Ref. 13 for specific lots; P130X properties reported for PX7.
[c]Reported in Ref. 14. No details on test procedure.
[d]Amoco product data sheet; strand tests.
[e]Hercules product data sheet; strand tests.
[f]PAA-resin strand test; 2 in. gauge length.
[g]Epoxy-resin strand tests; 6 in. gauge length.

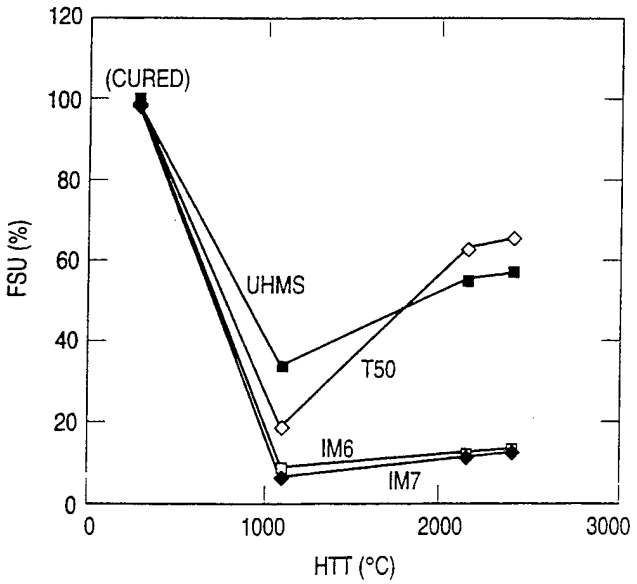

FIG. 2. Fiber strength utilization (FSU) versus heat-treatment temperature (HTT) for PAN-based fibers.

of the tow composite, and A_f is the (known) total cross-sectional area of the fibers in the tow. Fiber volume fractions were not measured, but, based on results of other studies,[15] were estimated to be in the range 0.25 to 0.40

Unlike before,[1] we have not carried the composite heat treatments to 2750 °C. At this high HTT, there was significant loss of composite strength for the E-series fibers due, most likely, to a combination of poor matrix stress transfer and *in situ* fiber damage as mentioned earlier. In addition, all of the PAN-based fiber composites except T50 experienced significant warping when heated to 2750 °C.

Calculation of FSU at each HTT for the E-series fibers was based on actual measured strengths of bare fibers heat-treated to the same HTT's. The heat-treated fibers were tested in epoxy-impregnated strands (see Fig. 2 of Ref. 1). For the three Amoco pitch-based fibers, we used the as-received strengths for all HTT, based on the results of Schulz,[16] which showed that the strengths of the P55 and P100 fibers were essentially unchanged by heat treatment to 2500 °C. It is known that the PX7 fibers have seen HTT's in excess of 2500 °C, so we can reasonably expect the same behavior as with the P55 and P100 fibers. For the PAN-based fibers, we also used the as-received strengths throughout. In previous work,[2] we measured a strength decrease of about 7% for T50 fibers following HTT to 2400 °C, and so we expect a comparable response with the UHMS fibers, which are also believed to be heat-treated to temperatures comparable to the T50. However, the strengths of the IM6 and IM7 most likely decrease significantly with HTT to 2400 °C because of a much lower initial HTT. As a result, the FSU's for the PAN-based fibers at 2400 °C, and particularly IM6 and IM7, represent lower-bound values.

Table III summarizes the results of Figs. 1 and 2, giving the values of fiber failure strain, strength, and strength utilization for each of the composites as a function of HTT. The fiber failure strains were calculated from the ratio of fiber strength to fiber modulus. The stress-strain curves for all the tow composites were linear to failure.

In Fig. 1, the E-series fiber results are those reported previously.[1] The P55 composites behave similarly to the E35, E75, and E105 composites, showing a large drop in FSU with carbonization to 1100 °C, followed by significant strength recovery with heat treatment to 2150 and 2400 °C. In contrast, the three very high-modulus-fiber composites, P100, PX7, and XN70, define a different pattern of behavior, showing steadily decreasing FSU with HTT to 2400 °C.

Figure 2 shows that the four PAN-based fibers behave similarly to the lower-modulus, pitch-based fiber composites of Fig. 1. The ultra-high strength IM6 and IM7 composites are remarkable in showing the lowest FSU for 1100 °C HTT (~8–9%) and no significant recovery of FSU with heat treatment to 2400 °C.

Low magnification SEM photos of fracture surfaces for the IM7 composites are shown in Fig. 3 for the cured-resin state (a), 1100 °C HTT (b), and 2400 °C HTT (c). Note the extreme flatness of the fracture surface for the 1100 °C HTT. Even with heat treatment to 2400 °C, there is still no extensive fiber pullout. The fracture surface shown in Fig. 3(a) was typical of all the PAN-based-fiber, cured-resin composites.

Figure 4 shows SEM photos of fracture surfaces for the 1100 °C and 2400 °C HTT UHMS composites. The increase in fiber pullout with HTT to 2400 °C is very marked and corresponds with a significant rise in FSU (Fig. 2).

Examining just the behavior of the pitch-fiber composites at the 1100 °C HTT, we see in Fig. 5 SEM photos of fracture surfaces for the P55, P100, and E130 composites. The P55 surface is typical of the groups of lower-FSU composites, showing matrix-dominated brittle fracture (see Fig. 4 of Ref. 1), with no fiber pullout. The uniquely behaving E130 composite reveals a rougher, more jagged surface, but very little distinct filament pullout. However, the P100 composite shows very distinct filament pullout, indicative of a weaker fiber-matrix interface than in the E130 composite. This same fracture behavior was also seen with the PX7 and XN70 composites.

TABLE III. Apparent fiber failure strains, strengths, and strength utilization (FSU) values for different composites by HTT (data for E35, E75, E105, and E130 are from Ref. 1).

Fiber	Failure strain (%), strength (GPa), and FSU (%)			
	Cured resin	1100 °C	2150 °C	2400 °C
E35	0.90	0.20	0.24	0.18
	2.1	0.5	0.6	1.4
	100	24	28	60
E75	0.40	0.09	0.21	0.22
	2.0	0.4	1.2	1.7
	100	24	62	74
E105	0.30	0.11	0.21	0.22
	2.1	0.7	1.5	1.8
	100	35	72	74
E130	0.25	0.22	0.24	0.21
	2.3	1.8	2.1	1.9
	100	79	92	68
PX7	0.25	0.17	0.13	0.11
	2.3	1.47	1.15	0.92
	100	64	50	40
P100	0.30	0.23	0.17	0.14
	2.2	1.67	1.17	1.10
	100	76	53	50
P55	0.48	0.08	0.27	0.15
	1.8	0.32	1.03	1.15
	100	18	57	62
XN70	0.30	0.18	0.18	0.17
	2.1	1.32	1.28	1.24
	100	63	61	59
IM6	1.85	0.16	0.20	0.22
	5.0	0.45	55	0.60
	100	9	11	12
IM7	2.0	0.16	0.22	0.24
	5.2	0.42	0.57	0.62
	100	8	11	12
UHMS	0.86	0.30	0.47	0.50
	3.6	1.26	1.98	2.08
	100	35	55	58
T50	0.63	0.12	0.40	. . .
	2.4	0.45	15	1.6
	100	19	63	66

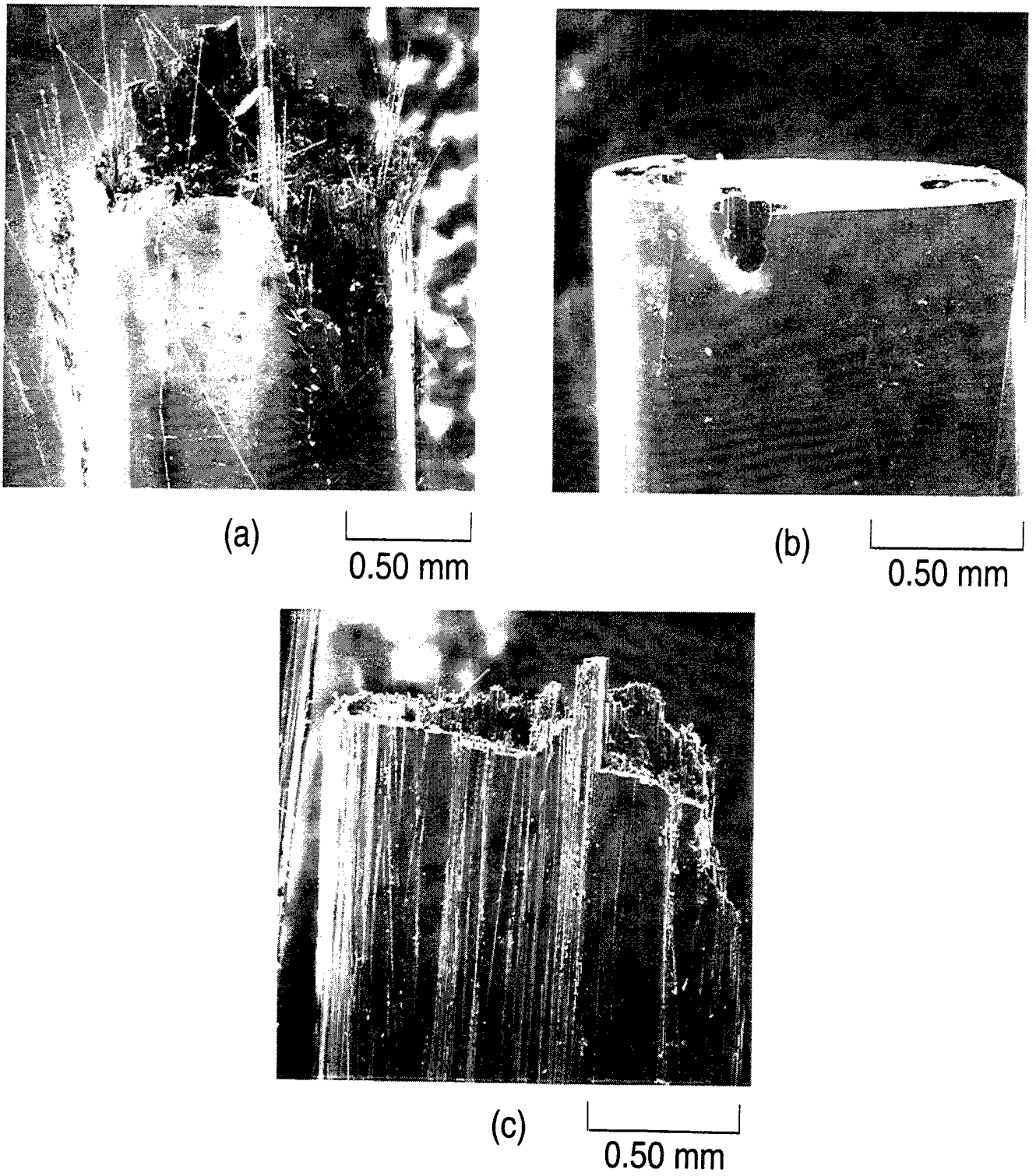

FIG. 3. Scanning electron micrographs of fracture surfaces of IM7 composites: (a) cured-resin, (b) 1100 °C HTT, and (c) 2400 °C HTT.

Figure 6 shows the fracture surfaces of these same three composites for the 2150 °C HTT. For both the P55 and E130 composite, there are modest increases in fiber pullout length and corresponding increases in FSU. But with the P100, PX7, and XN70 composites, pullout lengths are significantly larger (illustrated for P100) and correspond to decreasing FSU's. Note also the smooth fracture surfaces of the P55 and P100 fibers relative to

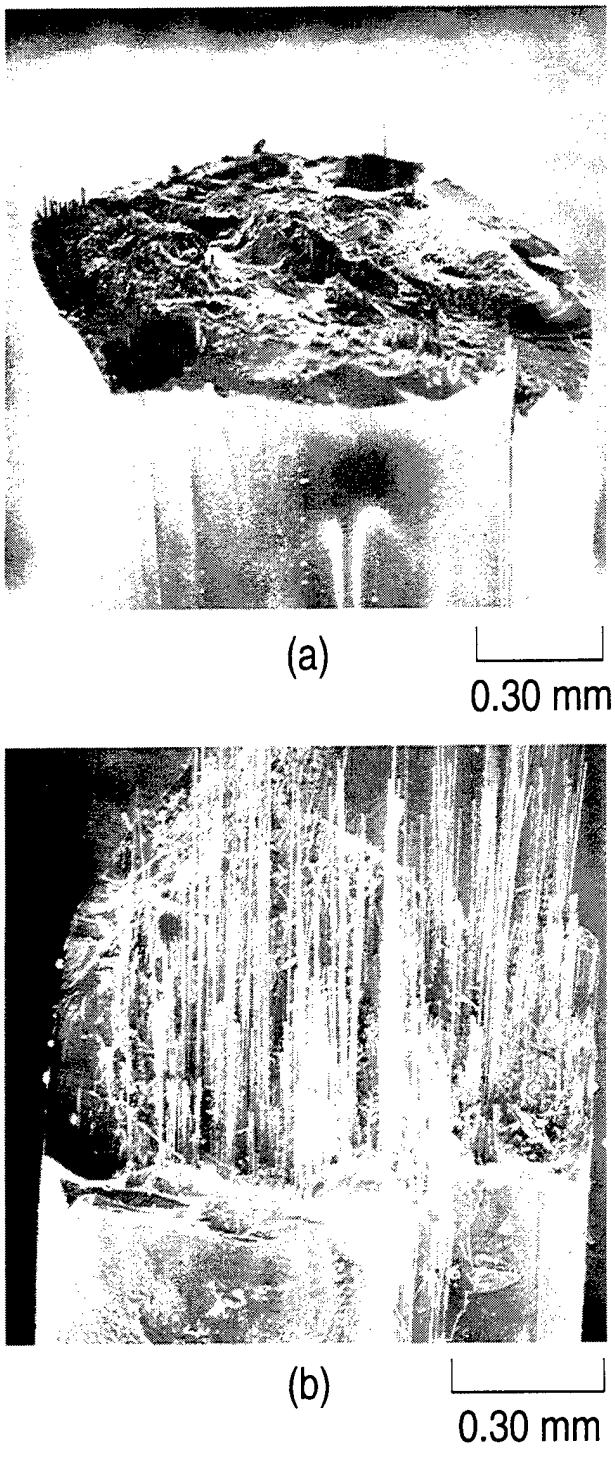

FIG. 4. Scanning electron micrographs of fracture surfaces of UHMS composites: (a) 1100 °C HTT and (b) 2400 °C HTT.

the spiny, jagged E130 fiber surfaces. Heat treatment to 2400 °C leads to still larger pullout lengths and lower FSU's for the P100, PX7, and XN70 composites.

The physical model that emerges from the SEM fractographs of Figs. 5 and 6 is one of an optimum fiber-matrix IFSS that balances the demands of crack deflection at a weakened interface with that of strong fiber-matrix adhesion, which is necessary for efficient crack-tip shielding and matrix shear-stress transfer in the vicinity of broken fiber ends. For the E130 composite, we would argue that an optimum IFSS is reached in the vicinity of the 2150 °C HTT, at which HTT the FSU is 92%. However, for the P100, PX7, and XN70 composites, the IFSS at 1100 °C HTT is already so low that further weakening of the IFSS with higher HTT's leads to strength values that are of the same order as dry fiber bundles. [For brittle filaments, which typically have strength variation from 10 to 20% (corresponding roughly to Weibull moduli of 6 and 12, respectively), we would expect dry bundle strength efficiencies to be about 0.65 to 0.80.[17]] In further contrast, the E35 composite remains well bonded, even with heat treatment to 2150 °C, and only heat treatment to 2400 °C results in sufficient weakening of the interface to produce a significant increase in FSU.

There are two mechanisms that work to reduce IFSS with increasing HTT. The first, and probably more significant, are the thermally induced stresses that develop in any anisotropic structure with heat treatment and subsequent cooldown. These stresses can lead to fiber-matrix debonds and reduced interfacial strength. A second factor, unique to C/C, is the phenomenon of stress-induced orientation and graphitization of the matrix zone around the fiber.[18] This graphitized zone, the precursor to which is formed during pyrolysis,[18] develops progressively with HTT, particularly above about 2100 °C, and does so with a decrease in volume (increase in density at constant mass). If the fiber and matrix are debonded, then the graphitized matrix zone will shrink away from the fiber, leaving in most cases a gap that is clearly visible by optical microscopy or SEM.[19]

We can take advantage of this latter effect to assess qualitatively the presence of fiber-matrix debonding following the higher HTT's. Figure 7 shows polarized-light micrographs of the four ultra-high-modulus fiber composites corresponding to heat treatment to 2750 °C. Although we did not measure FSU values at this high HTT for the additional fibers in this work, the matrix shrinkage and debonding is the most pronounced and best illustrated at this HTT. Graphitization of the matrix is extensive at 2750 °C and leads to the very striking micrographs showing the P100, PX7, and XN70 fibers lying unbonded in faceted matrix "holes" produced by polygonization of the graphitized matrix around these fibers. Similar observations, although less extensive in frequency and with smaller debond gaps, were seen in the micrographs of these same three fibers for the 2400 and 2150 °C HTT's. We observe at the same time that, unlike these three fibers, the E130 fiber remains well bonded even at 2750 °C in spite of a comparable

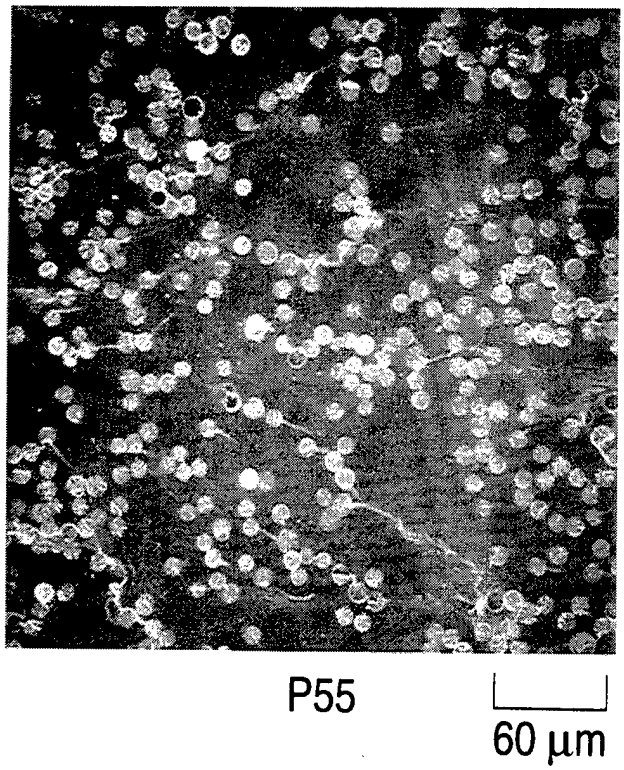

(a)

(b)

(c)

FIG. 5. Scanning electron micrographs of (a) P55, (b) P100, and (c) E130 composite fracture surfaces for 1100 °C HTT.

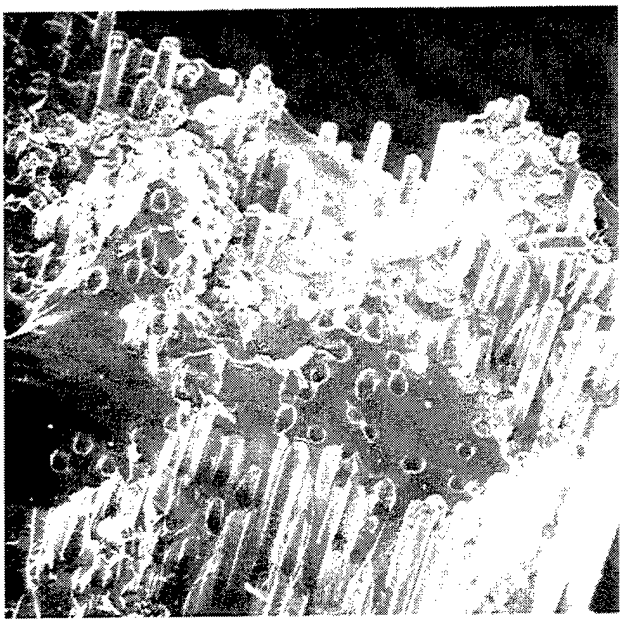

(a)

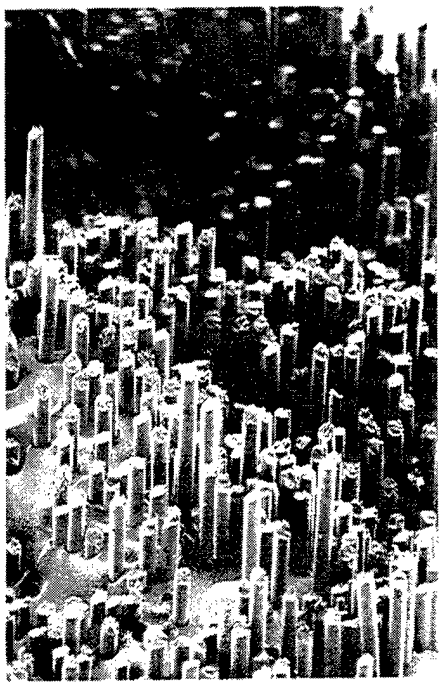

(b)

(c)

FIG. 6. Scanning electron micrographs of (a) P55, (b) P100, and (c) E130 composite fracture surfaces for 2150 °C HTT.

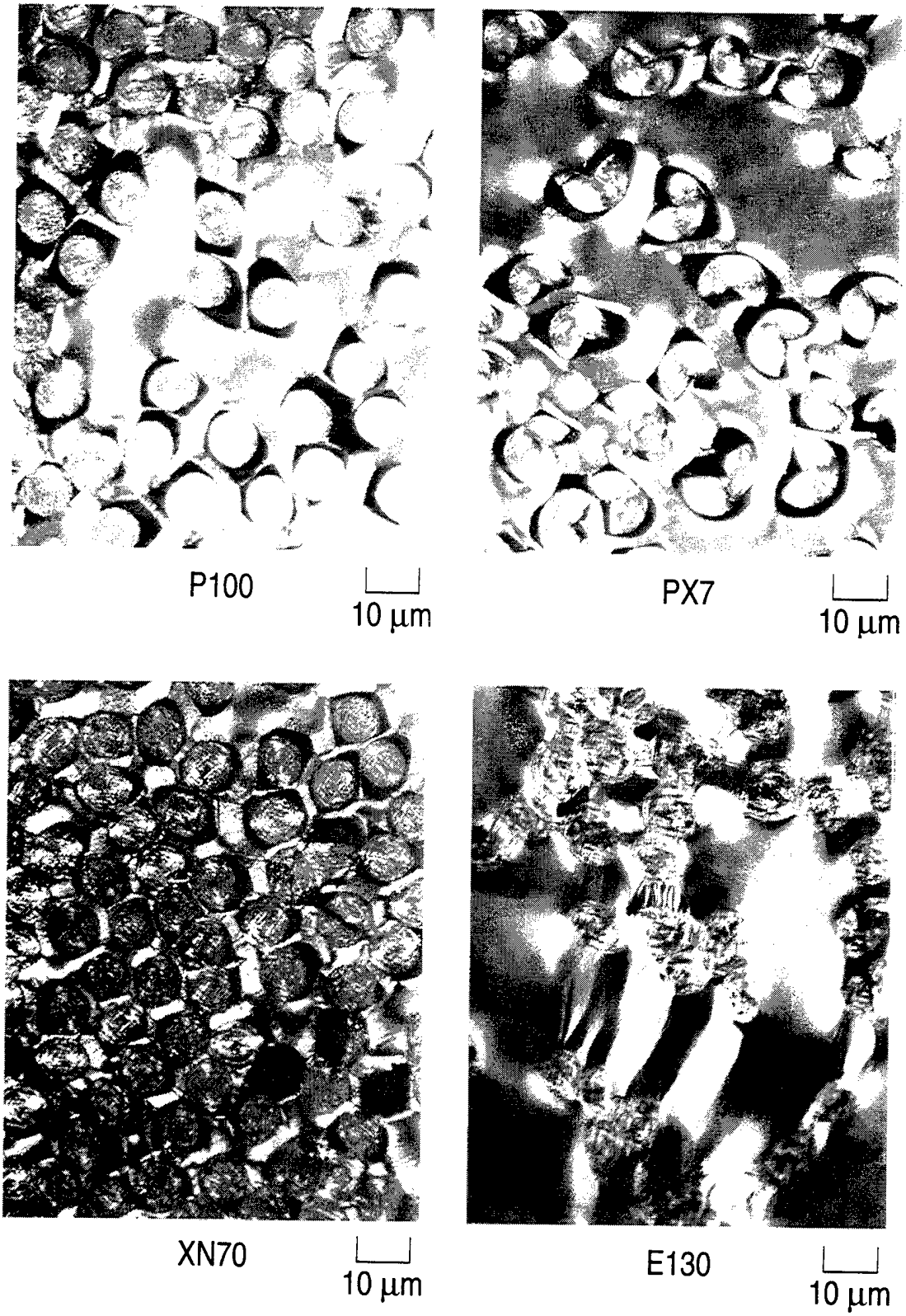

FIG. 7. Optical polarized-light micrographs of polished cross sections of P100, PX7, XN70, and E130 composites for 2750 °C HTT.

degree of matrix graphitization. Note also the much coarser optical extinction lines in the graphitized matrix zones between fibers for the E130 composites. Overall, it was found that extensive fiber-matrix debonding was observed only in the P100, PX7, and XN70 fiber composites.

Further evidence of fiber-matrix bonding and debonding can be seen in higher magnification SEM's of composite fracture surfaces illustrated in Fig. 8 for the P55 and P100 composites. Two of the photos show P55 composite fracture surfaces at two different magnifications, corresponding to HTT's of 2750 °C and 2400 °C. Note the stringers of matrix that are apparently still attached to the fiber following fracture. In contrast, the fractured P100 fibers seen in Fig. 8 show little evidence of attachment to the matrix. Similar observations were made for the PX7 and XN70 composites at these same HTT's. In an independent study of some of these same composites by transmission electron microscopy (TEM), Rellick and Adams[20] have observed what appears to be a fusion or interpenetration of matrix into the fiber surface in certain composites. However, as they pointed out,[20] it is very difficult to make any semiquantitative estimate of the extent of such fiber-matrix bonding in any composite using the TEM technique.

Estimates of the relative magnitudes of fiber-matrix bond strengths from SEM fractographs and optical microscopy are complemented by measurements of fiber orientation by XRD and of the IFSS in the polymer-matrix composite by the SFC fragmentation test using Eq. (2). Table IV summarizes the IFSS data for the different fibers studied. Figure 9 shows that the fiber modulus correlates very well with preferred orientation (FWHM), a feature of carbon fibers that is now well established.[21] A plot of IFSS versus fiber modulus for all the composites is presented in Fig. 10 and reveals two apparent families of behavior. For a given modulus, the PAN-based fibers and the E-series, pitch-based fibers have a higher value of IFSS than do the Amoco pitch-based fibers or XN70 fibers, suggesting a more "active" surface for the same modulus in the former group. The upper curve in Fig. 10 is drawn as an estimated best fit for the E-fibers only. However, as can be seen, the results for the PAN-based fibers are in good accord with this curve. As expected from Fig. 9, a plot of IFSS versus preferred orientation also reveals these two same families of behavior.

Figure 11 is a plot of the measured FSU for the most brittle condition, 1100 °C HTT, versus the measured IFSS of the as-received fibers. As a first approximation, possible effects of sizing and surface treatment have been ignored. In this case, the solid line connects the points for all the pitch-based fibers. In the very high-modulus-fiber regime, defined by XN70, PX7, P100, and E130, there is increasing FSU in the brittle matrix, with increasing polymer-matrix IFSS up to a maximum value (for this particular test) in the vicinity of about 15 MPa, after which further increase in IFSS results in a sharp drop in FSU and the brittle failure observed. This behavior is consistent with the model of an optimum interfacial shear strength suggested earlier based on micrographic observations. However, the apparent trend of increasing FSU with IFSS for the four high-modulus fiber composites, which defines the rising portion of the curve, may be fortuitous, given the narrow range of IFSS values and the uncertainties involved in this measurement. Nevertheless, the general trend of the data, showing increasing FSU with decreasing IFSS, appears clearly valid and is consistent with the proposed model.

We should also note that the data in Fig. 11 could be plotted in the same manner as in Fig. 10, with one curve connecting the points for the E-fibers, and a second, lower curve connecting the P-fibers and the XN70.

It is interesting that a measurement of IFSS in an epoxy resin matrix for a series of fibers would correlate meaningfully with the strength and fracture behavior of these same fibers in a *carbon* matrix, particularly when the carbon matrix precursor (PAA) is so different in structure from the epoxy matrix. Although both are thermosets, PAA is an almost totally aromatic polymer with no heteroatoms, whereas epoxy resin has a high oxygen content and is strongly polar. However, even if the same resin were used in the C/C as in the IFSS test, it is not obvious that the relative adhesion in the polymer-matrix composites should carry over to the thermally degraded (i.e., carbonized) matrices. That it appears to do so to a large degree, and in this case independent of polymer matrix type, suggests strongly that adhesion between carbon fibers and both the polymer and carbon matrix has less to do with chemistry than with some type of mechanical interlocking between fiber and matrix. This is the same conclusion reached by Harvey *et al.* [22] who have studied extensively the chemistry of the fiber surfaces using x-ray photoelectron spectroscopy (XPS). They measured interlaminar shear strengths (ILSS's) (using a short beam shear method) of composites fabricated with type 2 PAN-based carbon fibers and an epoxy resin. The fibers were subjected to a number of electrolytic surface treatments that resulted in significant increases in ILSS. Surface functionality on the fiber surfaces was followed by XPS. It was concluded that ILSS's of the composites were independent of the type and amount of surface functional groups and that most probably the observed increases in ILSS with surface treatment were the result of an improved mechanical keying of the resin to the fiber surface.

The final point of discussion is the apparent difference in bonding behavior between the E-series and P-series pitch-based fibers, suggested by the SEM fractographs and optical micrographs and the IFSS results presented in Fig. 10. Figure 12 shows SEM's of the transverse-section microstructures of the eight pitch-based carbon fibers. A number of these fibers have been extensively characterized by SEM and TEM previously.[13,23–25] The E-series fibers are characterized

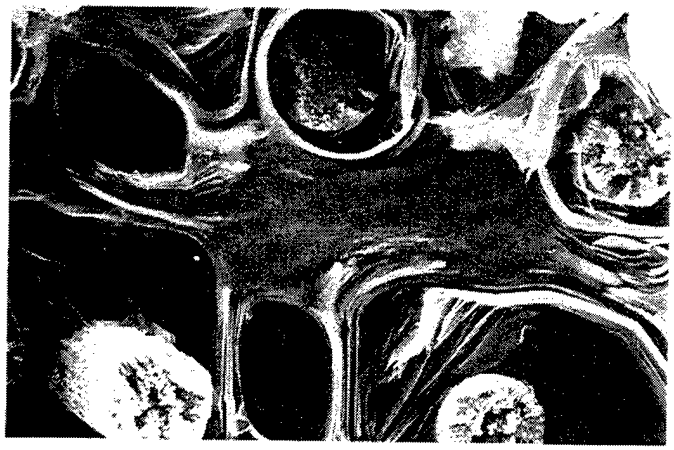

P55/2750°C

10 μm

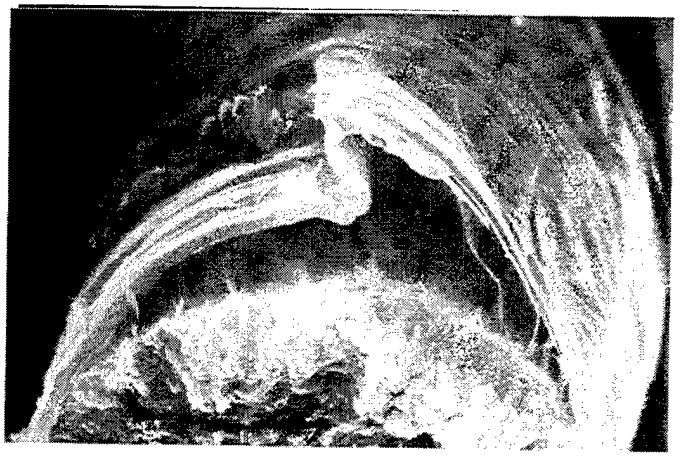

P55/2400°C

1 μm

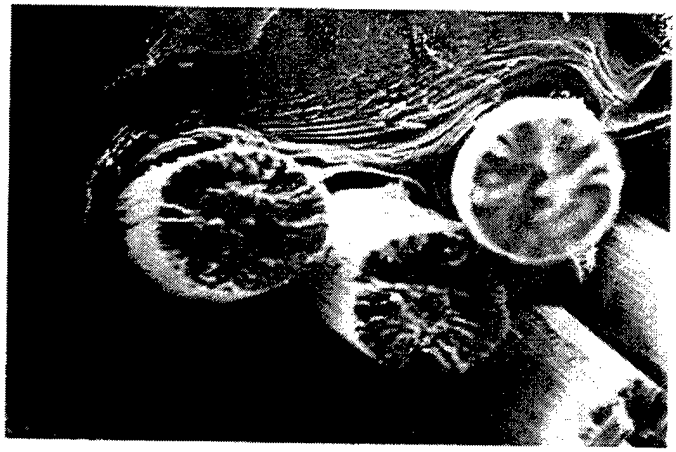

P100/2400°C

6 μm

FIG. 8. SEM's of fracture surfaces of P55 composites (HTT 2750 and 2400°) and P100 composites (2400 °C).

TABLE IV. Interfacial shear strengths (IFSS) of as-received fibers measured by single-fiber composite (SFC) fragmentation test.

Fiber	IFSS (MPa)
E35	34.5
E75	29.5
E105	19.5
E130	14.6
P55	23.5
P100	10.0
PX7	9.0
XN70	6.8
T50	30.0
UHMS	40.0
IM6	37.0
IM7	...

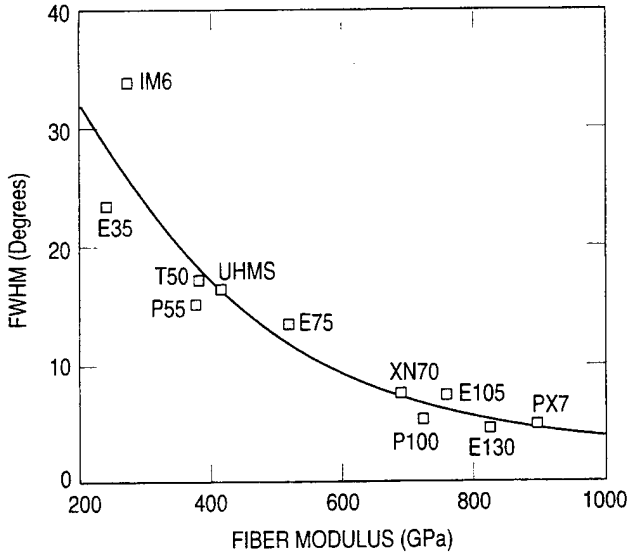

FIG. 9. Fiber preferred orientation (FWHM) versus fiber modulus.

principally by a radial zig-zag texture.[23] As the moduli of this series of fibers increase, the radial planes become somewhat sharper and better defined, but change little in their degree of waviness. The P55 fiber has a radial-type microstructure, while both the P100 and PX7 fibers reveal predominantly oriented-core microstructures.[13] Occasionally the PX7 fibers are found to have the open-wedge ("Pacman") structure (e.g., Fig. 7) with correspondingly strong radial texture. The XN70 fibers are more difficult to classify. Some have the oriented-core structure, while others (e.g., Fig. 12) show mostly a radial texture with some zig-zag character.

Some insight into the bonding behavior of these fibers may be gained by examining the work of Endo[24] on a series of Carbonic fibers from Kashima Oil Co. These fibers have a radial zig-zag structure similar to the E-series fibers from DuPont. In addition, the Carbonic HM60 and HM80 fibers had reported moduli of 84 and 112 Mpsi, which are comparable to those of

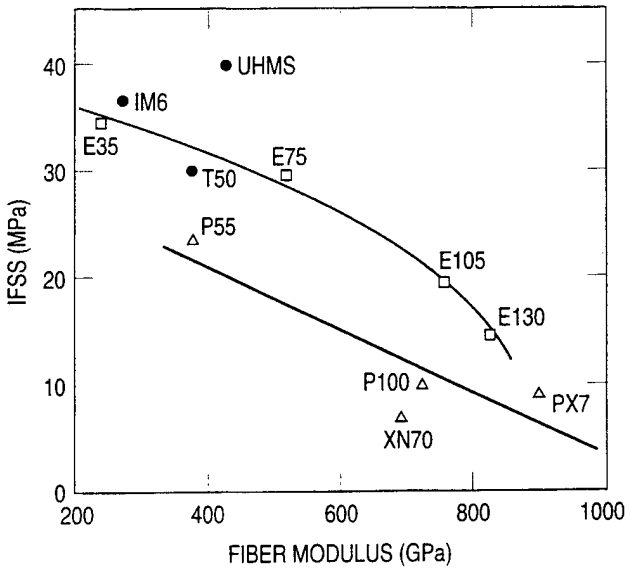

FIG. 10. Fiber-matrix interfacial shear strength (IFSS) as measured in an epoxy resin using single fiber composite (SFC) fragmentation test versus fiber modulus.

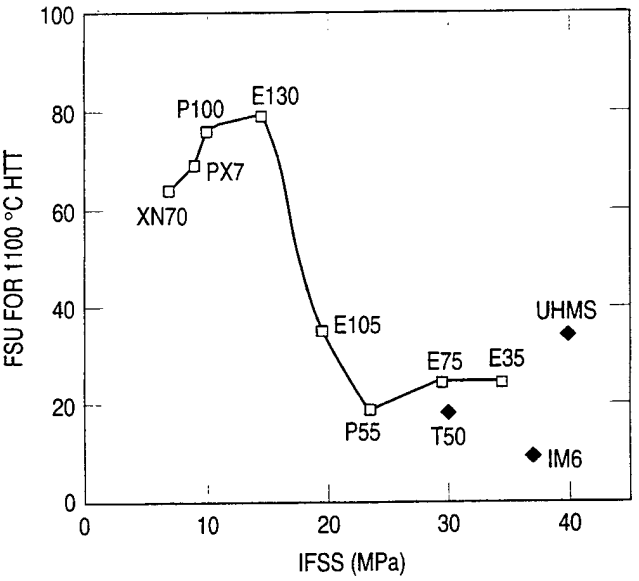

FIG. 11. Fiber strength utilization for 1100° HTT versus IFSS.

the E75 and E105 fibers. From TEM studies, Endo argued that the fine structure of the Carbonic fibers was much more like that seen in high-modulus PAN-based fibers than in conventional mesophase-based fibers such as the P100 and P120, which he also studied. This observation was supported by measurements of transverse magnetoresistivity of fibers, which showed positive magnetoresistivity for the P100 and P120 fibers and negative magnetoresistivity for the Carbonic fibers. Even with heat treatment to 2850 °C, the magnetoresistivity of the Carbonic fiber HM50 (modulus of 70 Mpsi) remained negative. The interpretation of these results

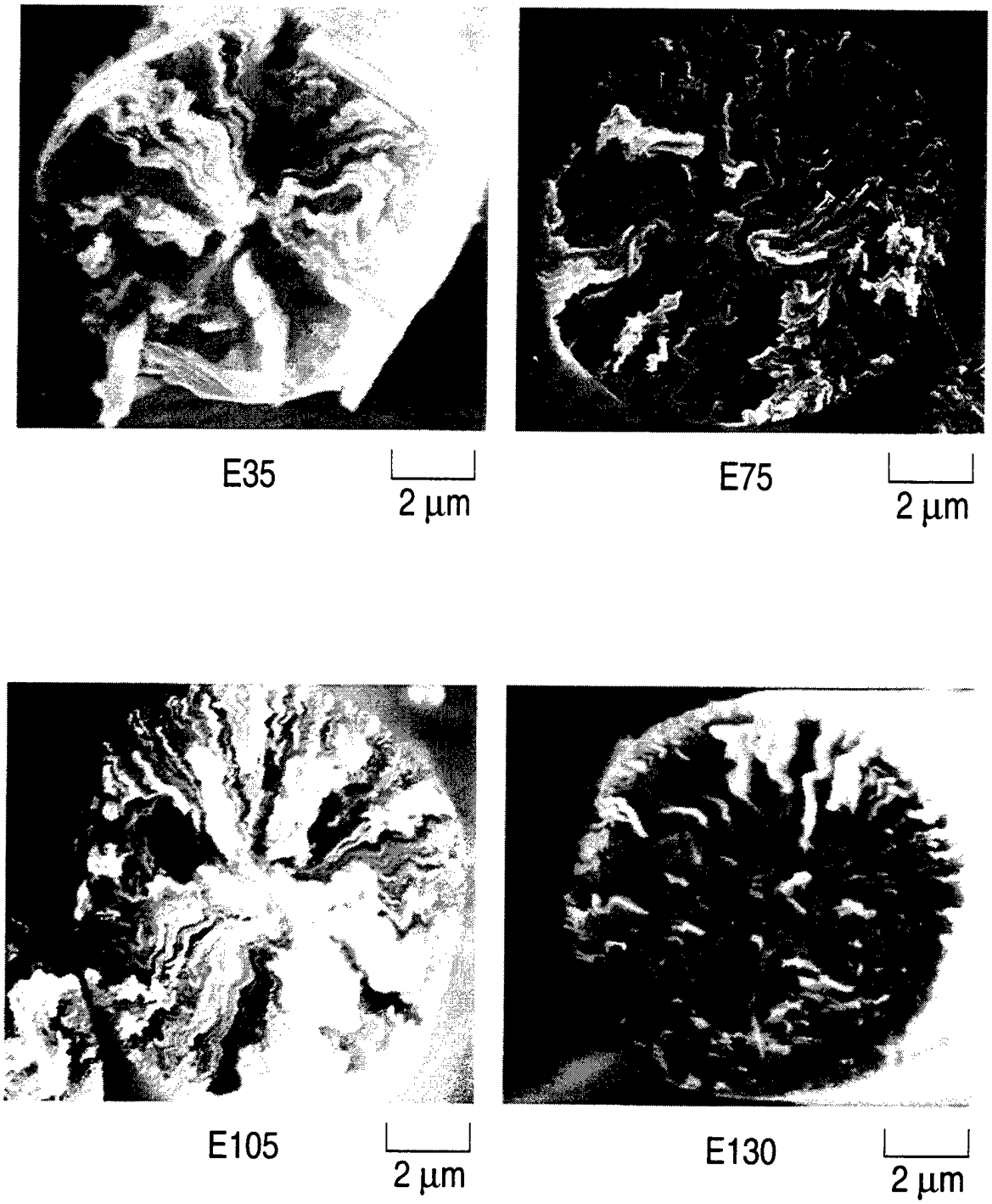

FIG. 12. Microstructures of pitch-based fibers as seen by SEM's of transverse fracture surfaces: E35, E75, E105, E130, P55, P100, PX7, and XN70.

is that the Carbonic fibers have a turbostratic structure, while the P-fibers are composed mainly of three-dimensional graphitic structure.

In another study, Hoffman,[26] using scanning tunneling microscopy (STM), has also remarked on the similarity in nanometer-scale surface structure of E-fibers, including E130 and PAN-based fibers.

IV. CONCLUSIONS

Results of this study show that the fracture behavior of unidirectional, single-tow C/C composites made with a variety of pitch- and PAN-based fibers is dominated by the interfacial shear strength (IFSS). This is inferred from SEM observations of fiber pullout at fracture surfaces and by optical microscopy of polished cross

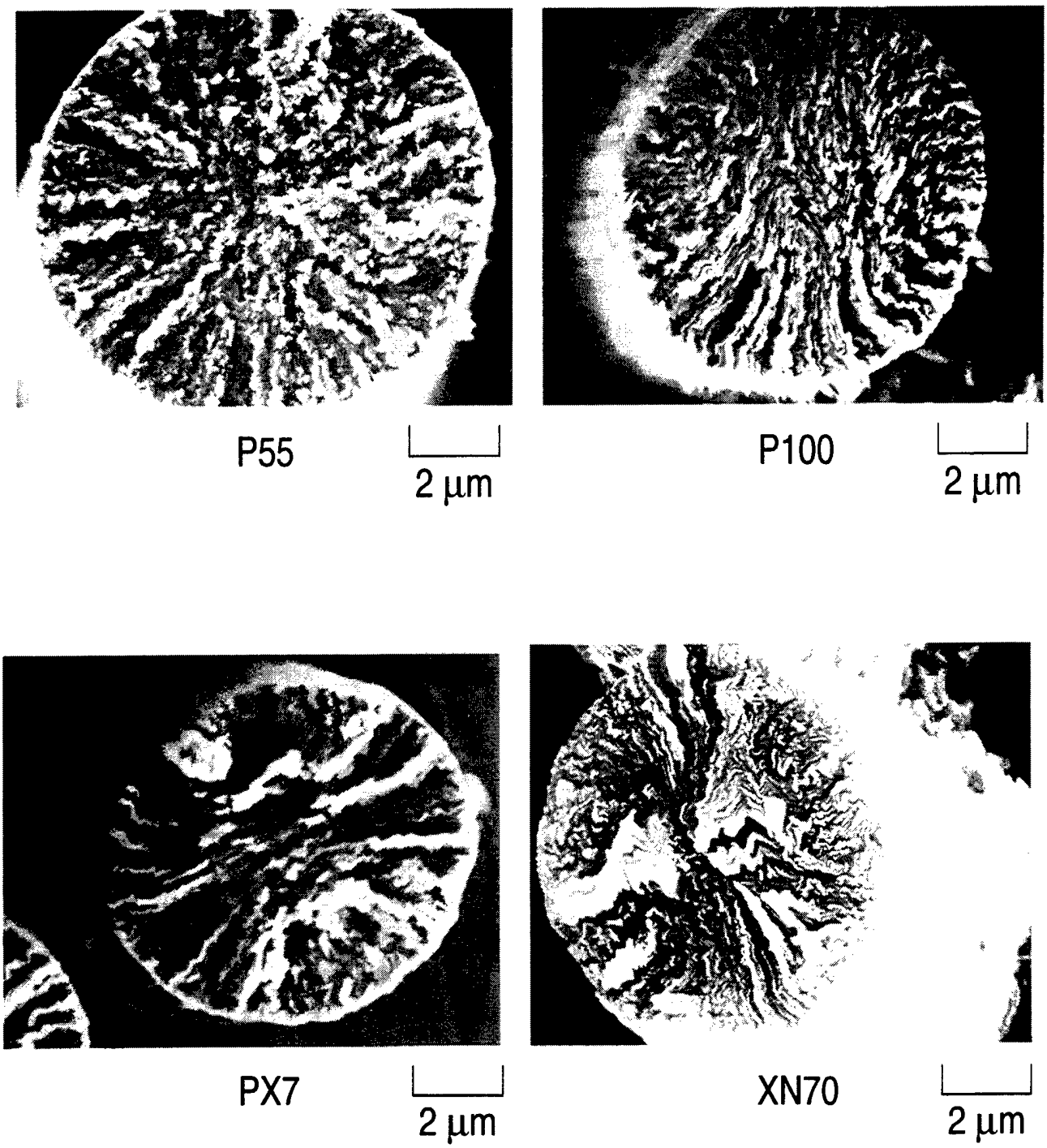

FIG. 12. (*continued*)

sections. These observations are further supported by measurements of IFSS for each of the fibers in an epoxy matrix using the single-fiber-composite (SFC) fragmentation test.

From the SFC test, it is found that there is no simple relationship between either the fiber modulus or degree of orientation and the IFSS. In particular, for the pitch-based fibers, the E-series fibers, as a function of modulus, define a family with higher IFSS than for the PAN-based fibers, the P-series fibers, and the XN70 fiber. The greater IFSS in the PAN-based and E-series fibers, as measured in the epoxy resin, is translated, or carried over, to the C/C at the various HTT's up to the maximum HTT of 2400 °C. This is inferred from the observation

of fracture surfaces by SEM and optical microscopy. In contrast, the P-series fibers and the XN70, which revealed weaker bonding at 1100 °C HTT, show even more extensive debonding at the higher HTT's of 2150 and 2400 °C. Since the polyarylacetylene (PAA) resin matrix precursor used for the C/C's is very dissimilar in structure compared to an epoxy resin, the initial bonding, as well as the carryover of bonding to the C/C realm, suggests that fiber-matrix bonding may have less to do with chemistry of the fiber surfaces and more than with mechanical interlocking between fiber and matrix.

The weaker bonding with the very high-modulus P-series fibers and XN70 is manifested at the lowest HTT of 1100 °C by significant fiber pullout and, as a consequence, higher fiber strength utilization (FSU). Heat treatment to 2150 and 2400 °C weakens this bond further, and, as a result, there is a uniform decrease in FSU as the matrix becomes less capable of transferring load to the fibers.

In contrast, with the very high-modulus E130 fiber, bonding is clearly better so that further weakening of the fiber-matrix bond with HTT to 2150 °C is tolerated and, in fact, results in a significant increase in FSU. Similar strength recovery with HTT to 2150 or 2400 °C is seen with all the remaining fibers, which include all four PAN-based fibers and the P55 and E105 fibers. In addition, since all these latter fibers are well bonded at 1100 °C HTT, they experience matrix-dominated brittle fracture and low FSU. The strength recovery with heat treatment of this group of fibers, and the E130 fiber, suggests an optimum IFSS for each composite for controlling tensile strength.

The difference in bonding between pitch-based E-series and P-series fibers is of considerable interest, but the reason for this behavior remains unclear. Insight into possible mechanisms of bonding is suggested by the work of Endo[24] and Hoffman,[26] both of whom have noted the similarity in structure of the pitch-based E-series fibers and high-modulus PAN-based fibers.

REFERENCES

1. R.J. Zaldivar, G.S. Rellick, and J.M. Yang, J. Mater. Res. **8**, 501–511 (1993).
2. R.J. Zaldivar, G.S. Rellick, and J.M. Yang, SAMPE J. **27**, 29–36 (Sept/Oct 1991).
3. R.J. Zaldivar, R.W. Kobayashi, G.S. Rellick, and J.M. Yang, Carbon **29**, 1145–1153 (1991).
4. R.J. Zaldivar, G.S. Rellick, and J.M. Yang, in *Extended Abstracts, 21st Biennial Conference on Carbon,* Buffalo, NY (1993), pp. 52–53.
5. J. Aveston, G. Cooper, and A. Kelly, in *The Properties of Fiber Composites,* Conf. Proc. (NPL, IPC Science and Tech. Press, 1971), pp. 15–26.
6. D.B. Marshall and A.G. Evans, J. Am. Ceram. Soc. **68** (5), 225–231 (1985).
7. M.W. Barsoum, P. Kangutkar, and A.S.D. Wang, Compos. Sci. Technol. **55**, 257 (1992).
8. A. Kelly and W.R. Tyson, J. Mech. Phys. Solids **13**, 329 (1965).
9. L.T. Drzal, M.J. Rich, J.D. Camping, and W.J. Park, 35th Annual Tech. Conf. Reinforced Plastics/Composites Inst., Society of Plastics Indus., paper 20-C (1980).
10. L.T. Drzal and P.J. Herrera-Franco, in *Engineered Materials Handbook, Vol. 3* (ASM INTERNATIONAL, Materials Park, OH, 1991), p. 391.
11. P.J. Herrara-Franco and L.T. Drzal, Composites **23**, 2 (1992).
12. J.J. Mallon and P.M. Adams, Mol. Cryst. Liq. Cryst. **231**, 69 (1983).
13. J.D. Fitzgerald, G.M. Pennock, and G.H. Taylor, Carbon **29**, 139 (1991).
14. S-S. Lin, U.S. Army Materials Technology Laboratory, Report MTL TR-89-35, April 1989.
15. G.S. Rellick and R.J. Zaldivar, in *Extended Abstracts, 21st Biennial Conf. on Carbon,* Buffalo, NY (1993), pp. 68–69.
16. D.A. Schulz, in *Extended Abstracts, 18th Biennial Conf. on Carbon,* Worcester, MA (1987), pp. 16–17.
17. E. Scala, *Analysis of the Test Methods for High Modulus Fibers and Composites, ASTM STP 521* (ASTM, 1973), pp. 390–409.
18. G.S. Rellick, D.J. Chang, and R.J. Zaldivar, J. Mater. Res. **7**, 2798–2809 (1992).
19. R.J. Zaldivar and G.S. Rellick, *Carbon* **29**, 1155–1163 (1991).
20. G.S. Rellick and P.M. Adams, *Carbon* **32**, 127 (1994).
21. M.S. Dresselhaus, G. Dresselhaus, K. Sugihara, I.L. Spain, and H.A. Goldberg, *Graphite Fibers and Filaments* (Springer-Verlag, Berlin, 1988).
22. J. Harvey, C. Kozlowski, and P.M.A. Sherwood, J. Mater. Sci. **22**, 1585 (1987).
23. G.M. Pennock, G.H. Taylor, and J.D. Fitzgerald, Carbon **31**, 591 (1993).
24. M. Endo, J. Mater. Sci. **23**, 598 (1988).
25. M. Guignon and A. Oberlin, Fiber Sci. Technol. **25**, 231 (1986).
26. W.P. Hoffman, in *Extended Abstracts, 21st Biennial Conf. on Carbon,* Buffalo, NY (1993), pp. 112–113.

TECHNOLOGY OPERATIONS

The Aerospace Corporation functions as an "architect-engineer" for national security programs, specializing in advanced military space systems. The Corporation's Technology Operations supports the effective and timely development and operation of national security systems through scientific research and the application of advanced technology. Vital to the success of the Corporation is the technical staff's wide-ranging expertise and its ability to stay abreast of new technological developments and program support issues associated with rapidly evolving space systems. Contributing capabilities are provided by these individual Technology Centers:

Electronics Technology Center: Microelectronics, VLSI reliability, failure analysis, solid-state device physics, compound semiconductors, radiation effects, infrared and CCD detector devices, Micro-Electro-Mechanical Systems (MEMS), and data storage and display technologies; lasers and electro-optics, solid state laser design, micro-optics, optical communications, and fiber optic sensors; atomic frequency standards, applied laser spectroscopy, laser chemistry, atmospheric propagation and beam control, LIDAR/LADAR remote sensing; solar cell and array testing and evaluation, battery electrochemistry, battery testing and evaluation.

Mechanics and Materials Technology Center: Evaluation and characterization of new materials: metals, alloys, ceramics, polymers and composites; development and analysis of advanced materials processing and deposition techniques; nondestructive evaluation, component failure analysis and reliability; fracture mechanics and stress corrosion; analysis and evaluation of materials at cryogenic and elevated temperatures; launch vehicle fluid mechanics, heat transfer and flight dynamics; aerothermodynamics; chemical and electric propulsion; environmental chemistry; combustion processes; spacecraft structural mechanics, space environment effects on materials, hardening and vulnerability assessment; contamination, thermal and structural control; lubrication and surface phenomena; microengineering technology and microinstrument development.

Space and Environment Technology Center: Magnetospheric, auroral and cosmic ray physics, wave-particle interactions, magnetospheric plasma waves; atmospheric and ionospheric physics, density and composition of the upper atmosphere, remote sensing, hyperspectral imagery; solar physics, infrared astronomy, infrared signature analysis; effects of solar activity, magnetic storms and nuclear explosions on the earth's atmosphere, ionosphere and magnetosphere; effects of electromagnetic and particulate radiations on space systems; component testing, space instrumentation; environmental monitoring, trace detection; atmospheric chemical reactions, atmospheric optics, light scattering, state-specific chemical reactions and radiative signatures of missile plumes, and sensor out-of-field-of-view rejection.